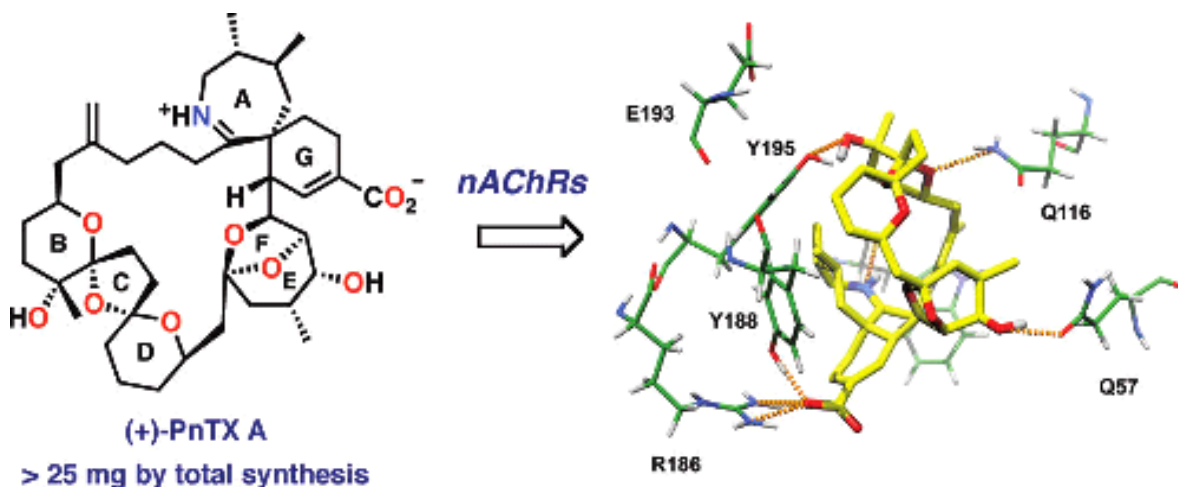


## Total synthesis of Pinnatoxins A.



### Contents

1. History & Introduction
2. Total Synthesis Of Pinnatoxin A
  - 2-1 Y.Kishi's Strategy
  - 2-2 A.Zakarian's Strategy
3. Revision of the Mode of Action of Pinnatoxin A
4. Summary

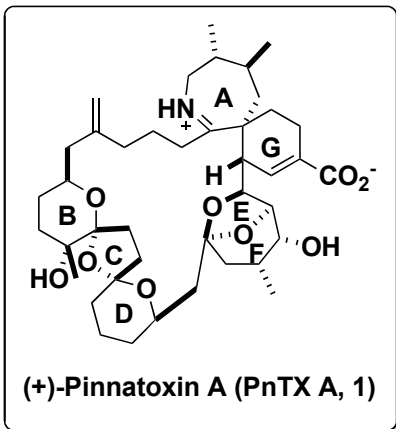
### History

- 1) Uemura and coworker isolated Pinnatoxin A from shellfish *Pinna muricata* in 1995.
- 2) Total synthesis of Pinnatoxin A

Y. Kishi -----	1998 ( <i>J. Am. Chem. Soc.</i> )
K. Nagasawa -----	2000 ( <i>J. Syn. Chem. Jap.</i> )
M. Inoue and M. Hiramata -----	2004 ( <i>Angew. Chem. Int. Ed.</i> )
S. Nakamura and S. Hashimoto ---	2008 ( <i>Angew. Chem. Int. Ed.</i> )
A. Zakarian -----	2011 ( <i>J. Am. Chem. Soc.</i> )



## Introduction

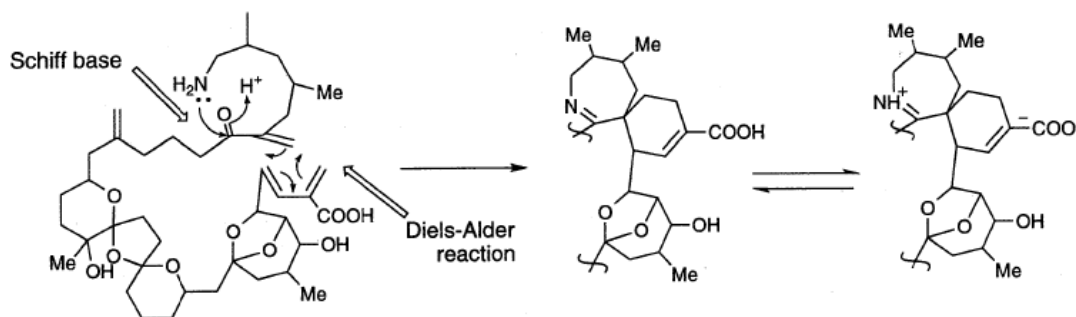


Pinnatoxin A, a marine toxin isolated from *Pinna muricata*, exhibits characteristic activity toward the  $\text{Ca}^{2+}$  channel.

Several unique structural features are

- (i) 27-membered carbocyclic framework,
- (ii) 19-membered polyether ring,
- (iii) 14 chiral centers,
- (iv) bis-spiroketal,
- (v) imminium and carboxylate functionality.

## Proposed biosynthesis of pinnatoxin A



⇒ This unique structure, which includes a 6,7-spiro ring (A and G rings), can be explained by the plausible biogenetic pathway shown here. This biogenesis does not involve the sequence of oxidation steps.

## Biological activities of Pinnatoxins

	acute toxicity of pinnatoxins in mice (LD <sub>50</sub> μg / MU)	P388 cytotoxicity of pinnatoxins (IC <sub>50</sub> μg / ml)
pinnatoxin A (1)	2.7	> 10
pinnatoxin B, C (2)	0.93	> 10
pinnatoxin D (3)	> 10	2.5

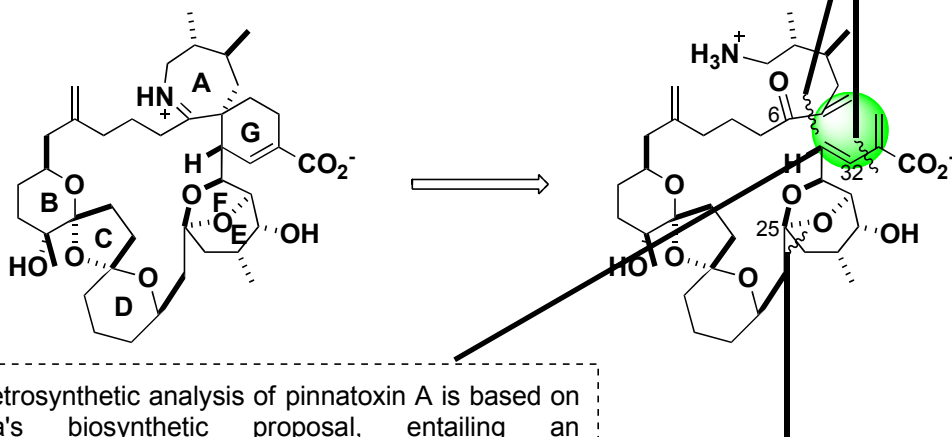
It has been initially suggested that the mode of action of pinnatoxins involves calcium-channel activation.

However, there is a growing body of evidence that different mechanism of activity may be operational.

# Kishi's Strategy

## Kishi's retrosynthetic analysis

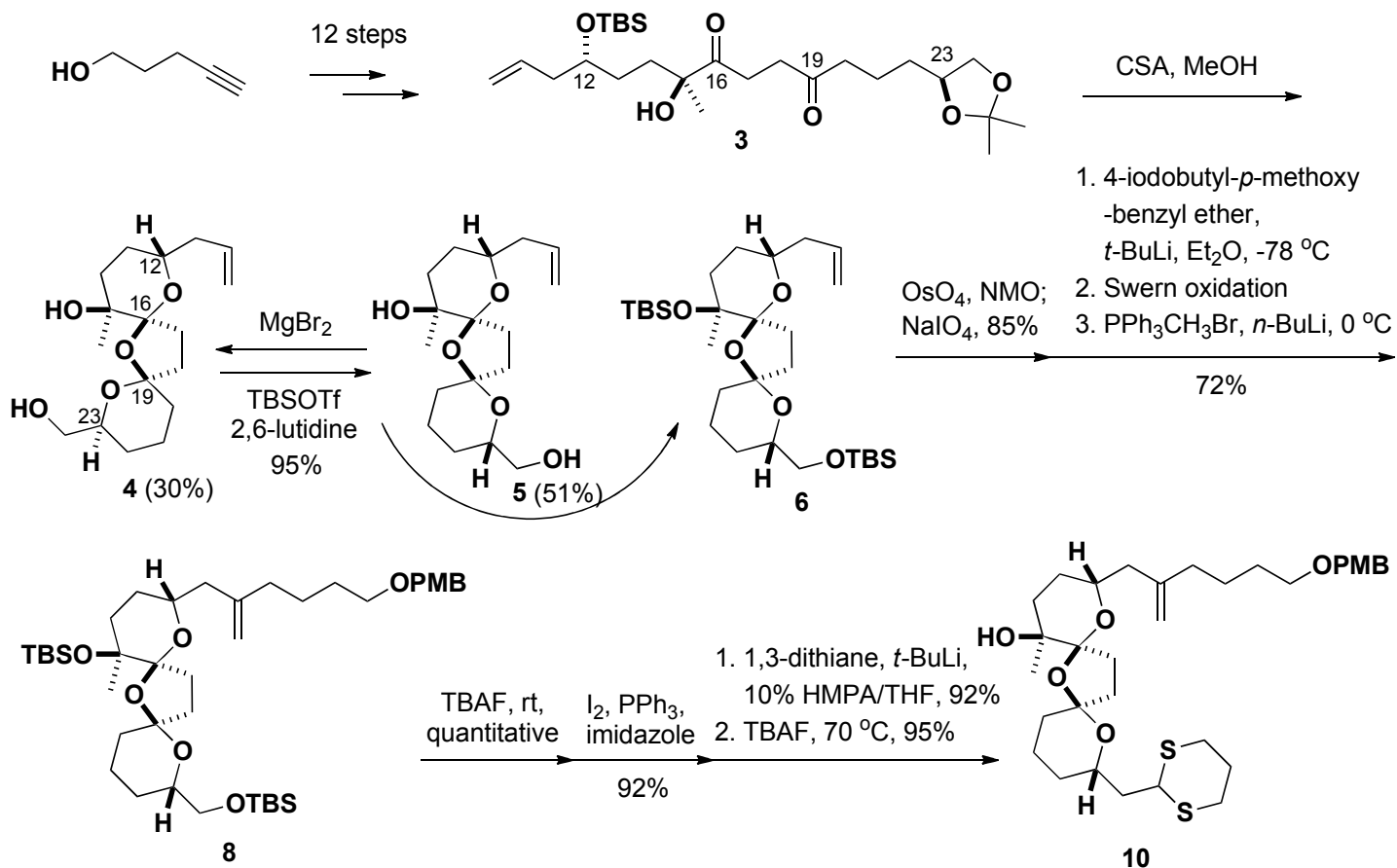
Ni(II)/Cr(II)-mediated couplings between vinyl iodides with C6 and C32 aldehydes.

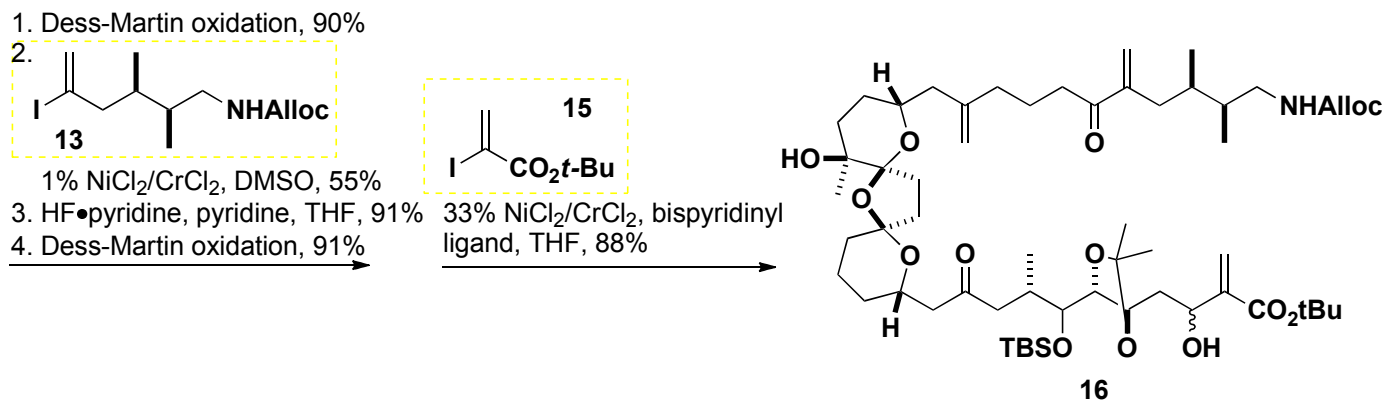
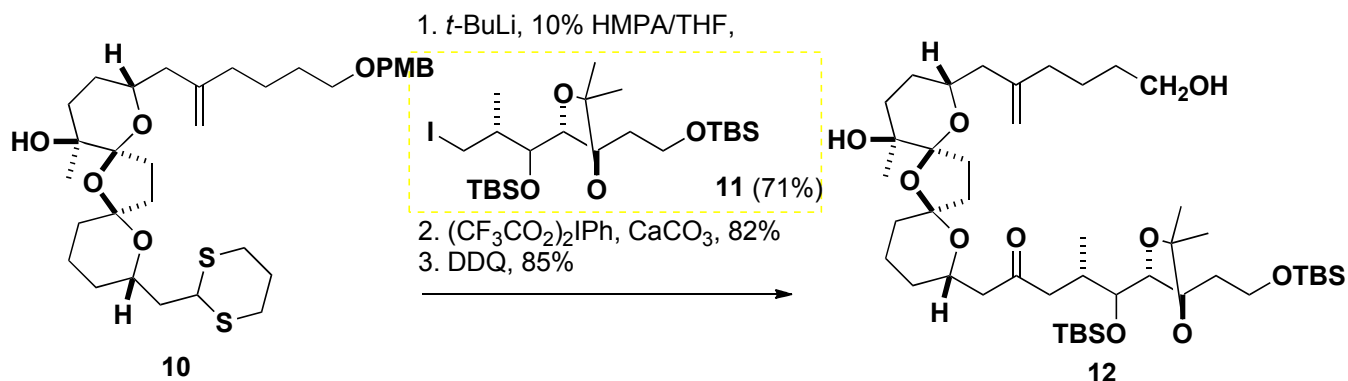


Their retrosynthetic analysis of pinnatoxin A is based on Uemura's biosynthetic proposal, entailing an **intramolecular Diels-Alder reaction** to construct the G-ring as well as the macrocycle, followed by imine formation to establish the 6,7-spiro-ring system.

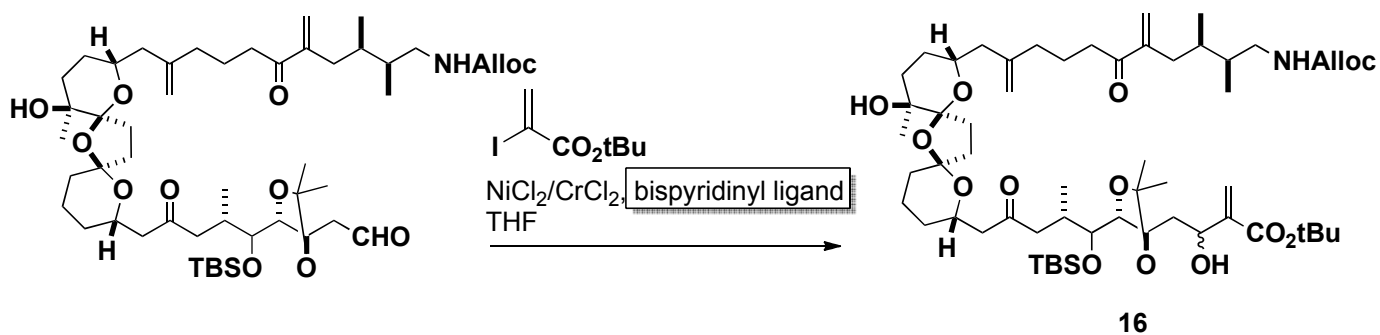
**Dithiane-based coupling** to form the C25-C26 bond.

## Construction of fragment 16



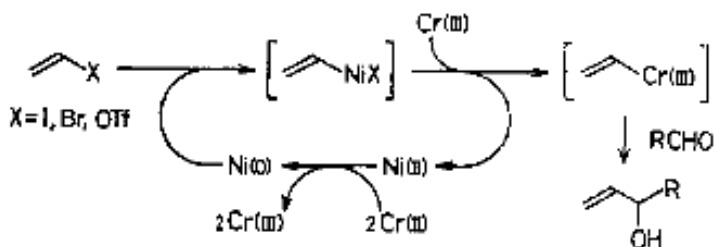


## Ni(II)/Cr(II)-Mediated Coupling Reaction



### • Catalytic cycle

Scheme I

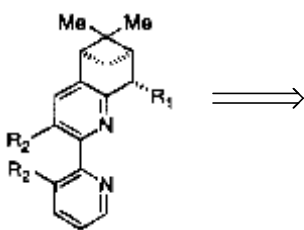


1) Nickel(II) chloride is first reduced to nickel(0) with 2 equiv of chromium(II) chloride.

2) Oxidative addition of alkenyl triflates to the nickel(0) takes place.

3) Then transmetalation reaction between the resulting alkenylnickel species and chromium(III) salt occurs to afford alkenylchromium reagents, which react with aldehydes to produce the desired allylic alcohols.

### •Bispyridinyl ligand



This process appears to involve the activation of the carbon-iodine bond via Ni(0) or Ni(I), the transmetalation of Ni to Cr, and the carbon-carbon bond formation via the organochromium reagent. A catalytic cycle of Ni is required for this process to function efficiently, suggesting that a chiral ligand for the current purpose must meet with the condition that its capacity to form metal complexes should not be too strong with Ni but should be sufficiently strong with Cr.

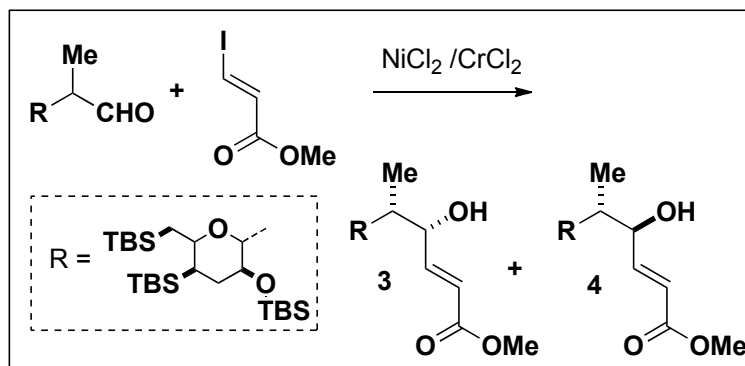


The homocoupling reaction was completely suppressed in the presence of these ligands. With a 1:2 mixture of NiCl<sub>2</sub> and CrCl<sub>2</sub>, the rate of coupling was dramatically enhanced, and reaction even at -20 °C became practical.

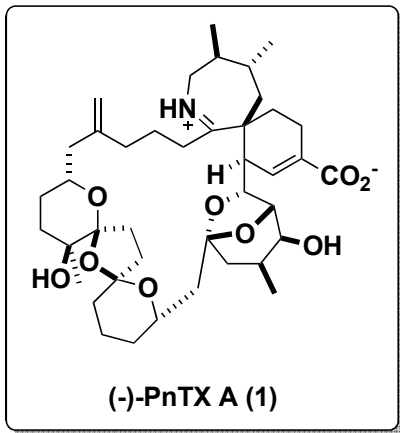
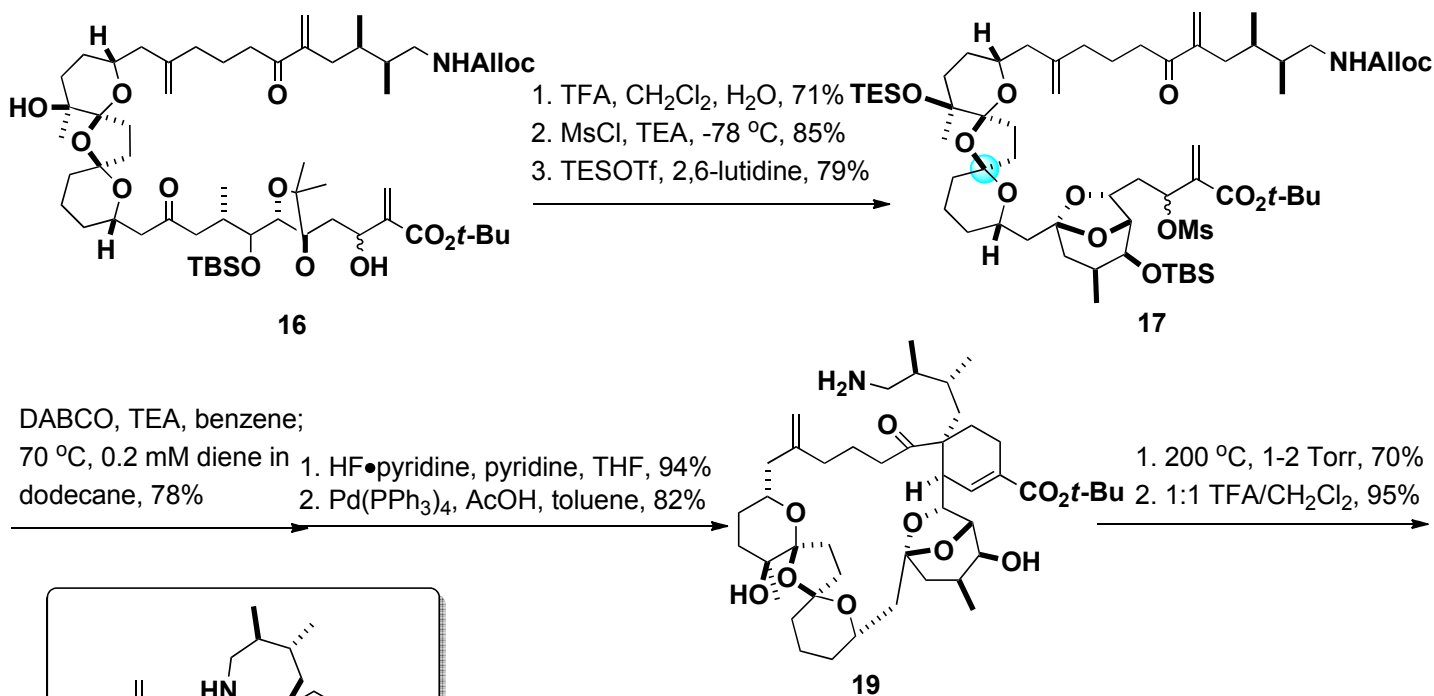
**Table 2. Solvents and Temperature Effects (for a representative coupling procedure, see ref 8)**

solvent	temp (°C)	time (h)	ratio (3:4) <sup>a</sup>
THF	30	1	4.2:1
	0	46	6:1
	-20	48	8-10:1
	40	48	a trace of products
Et <sub>2</sub> O	30	38	3.6:1
Ph <sub>2</sub> H	30	38	3.9:1
CH <sub>2</sub> Cl <sub>2</sub>	30	14	2.8:1
MeCN	30	14	3.3:1
DMF	30	24	no reaction
DMSO	30	24	no reaction

<sup>a</sup> The ratio of 3 and 4 was estimated from integrations of the resonances at 6.9 ppm (vinylic-H), 6.2 (vinylic-H), 4.5 (allylic-H), 1.2 (methyl-H) in the <sup>1</sup>H NMR spectrum.



### Construction of (-)-Pinnatoxin A

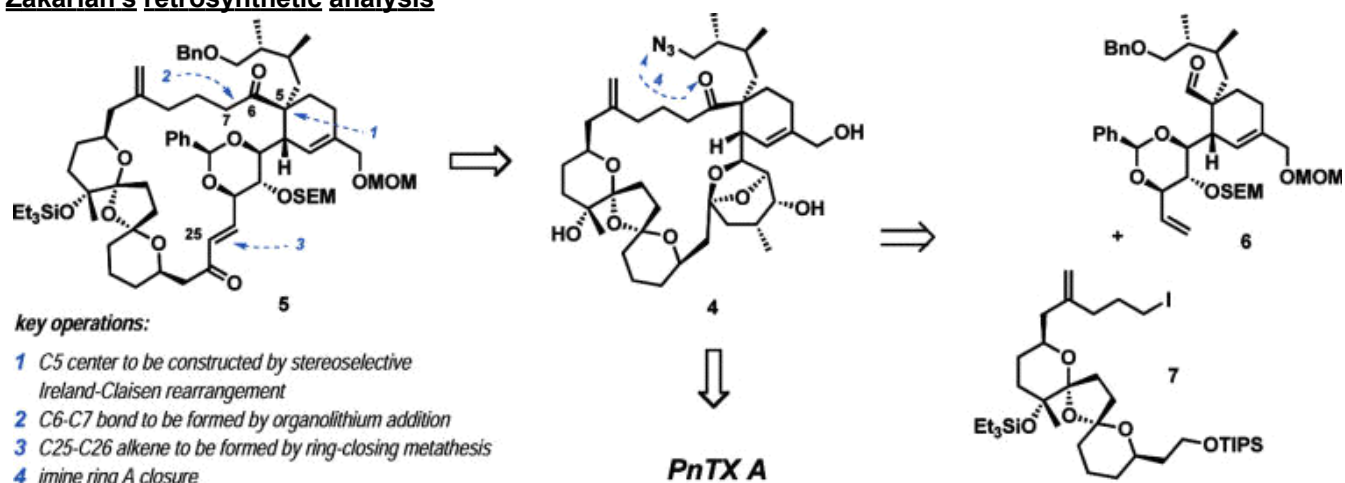


### Conclusion

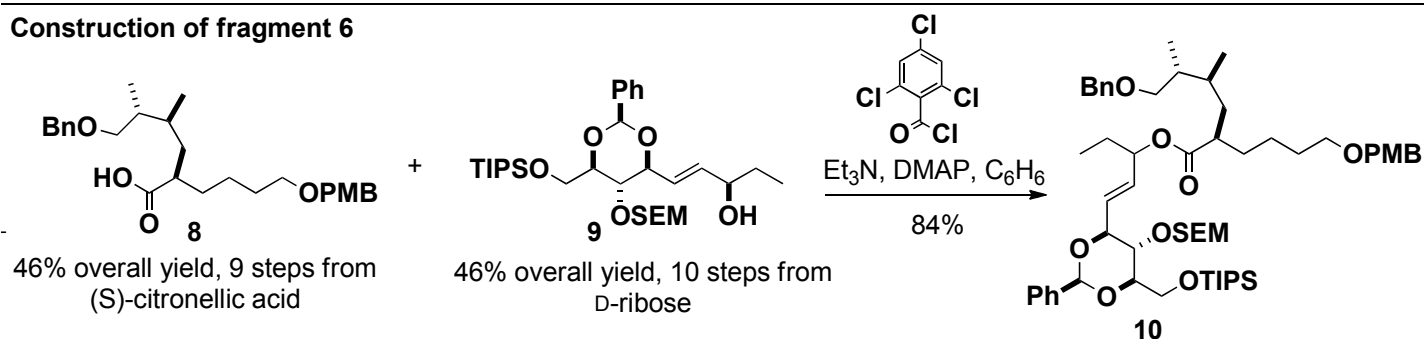
Kishi's group have completed the first total synthesis of pinnatoxin A utilizing a biomimetic intramolecular Diels-Alder reaction. This synthesis has also established the absolute stereochemistry of pinnatoxin A as the antipode of the structure 1.

# Zakarian's Strategy

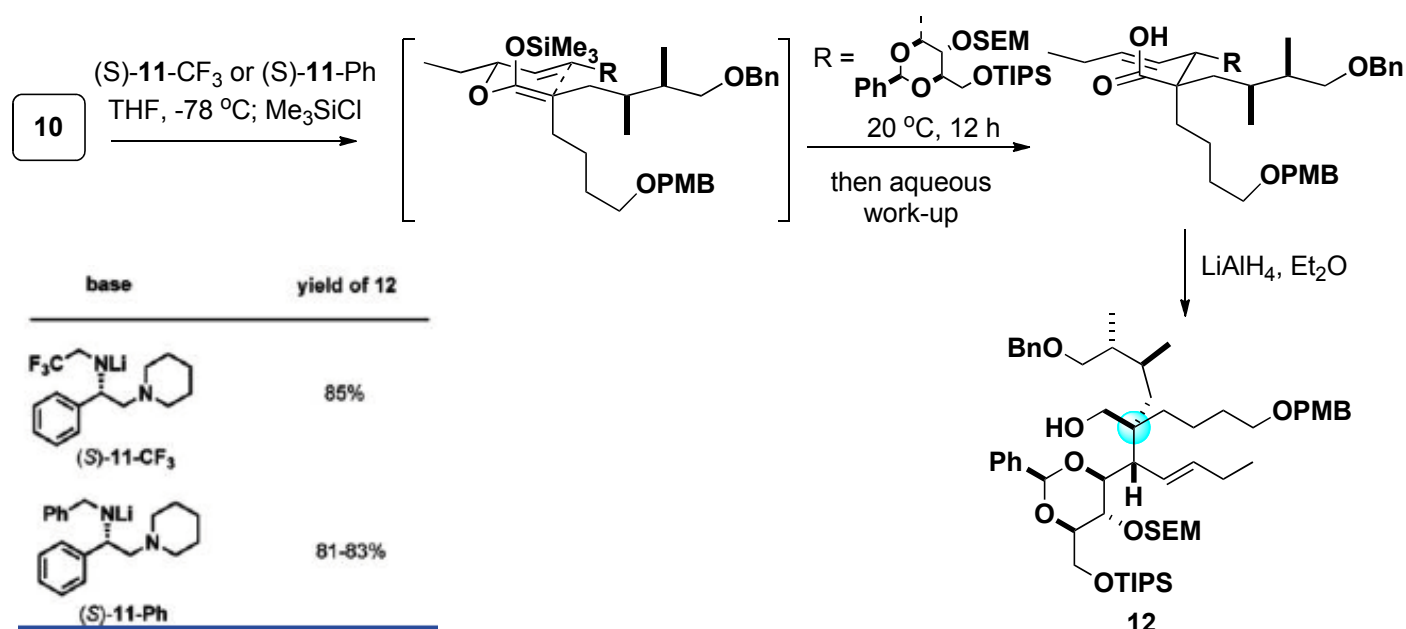
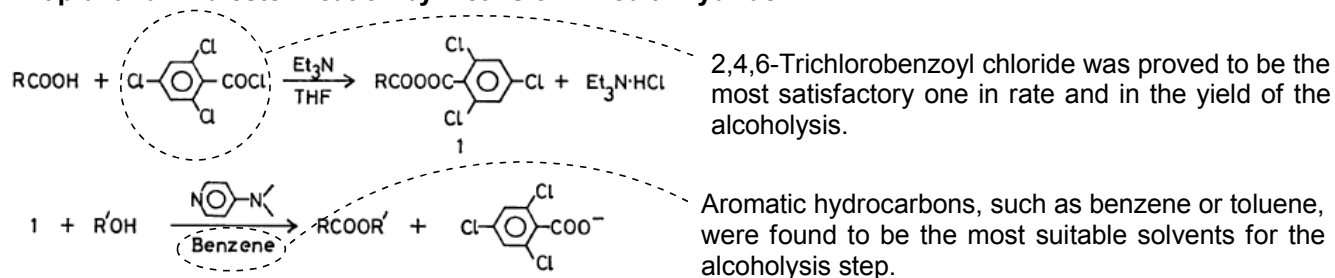
## Zakarian's retrosynthetic analysis



### Construction of fragment 6



### A rapid and mild esterification by means of mixed anhydride



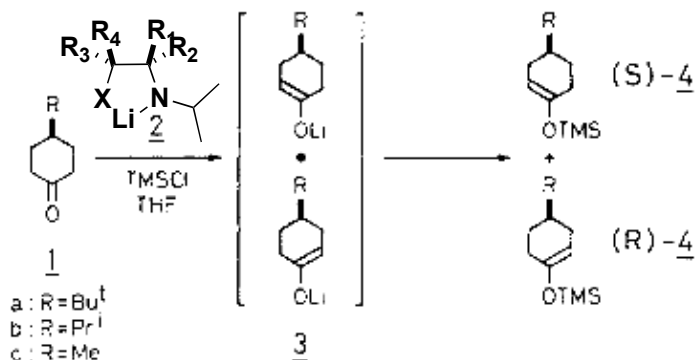
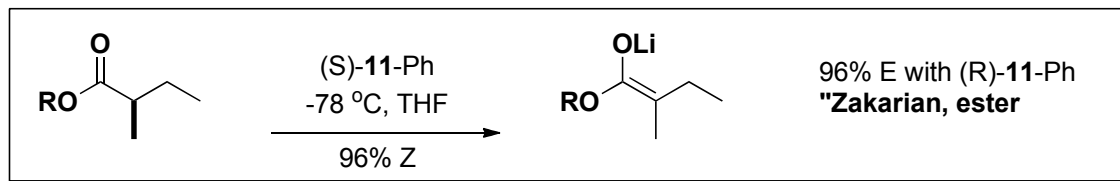
C5 center constructed.

6/16

## Highly stereoselective enolization of the acyclic $\alpha,\alpha$ -disubstituted ester.

### i) Enantioselective deprotonation by chiral lithium amide bases

A. Zakarian, *SYNLETT*, 2010, 11, 1717.  
K.Koga, *JACS*, 1986, 108, 543.



⇒ For deprotonation to occur by synchronous proton and lithium ion transfer, the carbonyl group in **1** will coordinate to the lithium from the same side as the lone pair.

#### [Characteristics of this chiral reagent]

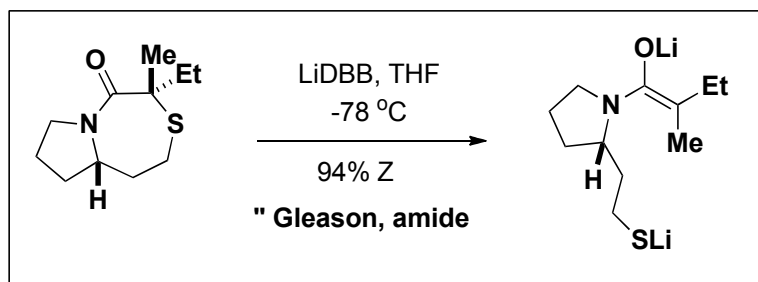


It is shown that the degree of asymmetric induction is highly dependent on the structures of chiral bases used and also on the bulkyness of the alkyl groups in cyclohexanones.

5-membered chelated structures are expected to be formed for the lithium amide as upward, where the isopropyl group on nitrogen should be exclusively trans to the bulky substitution on the chiral carbon for steric reasons. This infers that the direction of the lone pair on chiral nitrogen to be used for deprotonation is fixed.

### ii) Reductive enolate formation from bicyclic thioglycolate lactams

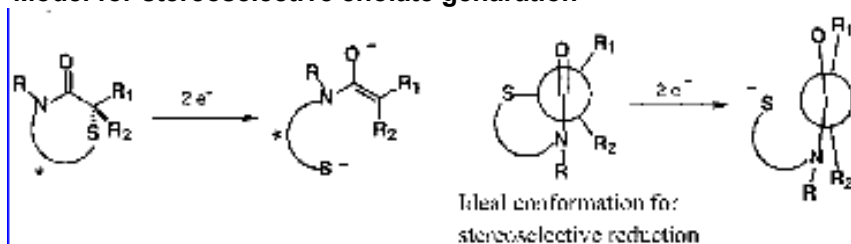
J. L. Gleason, *OL*, 2009, 11, 1725.  
J. L. Gleason, *JACS*, 2001, 123, 2092.



Highest levels of stereocontrol are usually associated with cyclic frameworks, while control based on differential steric environments is less reliable.

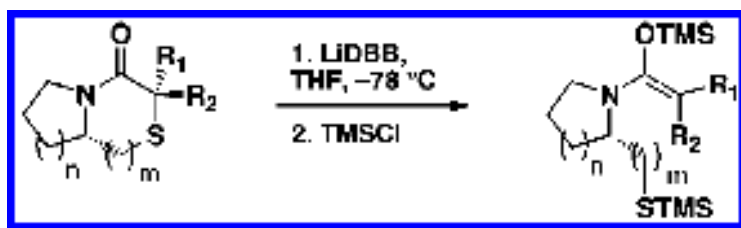
They report a method for controlling enolate geometry in disubstituted amide enolates where the *E/Z* selectivity is dependent only on the geometry and stereochemistry of the enolate precursor.

#### Model for stereoselective enolate generation



The design utilizes a two-electron reduction of  $\alpha,\alpha$ -dialkylated bicyclic thioglycolate lactams to provide disubstituted amide enolates.

## Reductive Enolization of Bicyclic Thioglycolate Lactams



Assuming that

- two alkyl groups ( $R_1$  and  $R_2$ ) are installed stereoselectively at  $\alpha$ -position,
- the O-C-C-S dihedral angle is held as close to  $90^\circ$  as possible by the bicyclic system, and
- significant bond rotation does not occur about the carbonyl-carbon/ $\alpha$ -carbon bond during the two-electron reduction process, the E/Z stereochemistry of the enolate should be controlled by the relative position of  $R_1$  and  $R_2$  in the starting lactam.

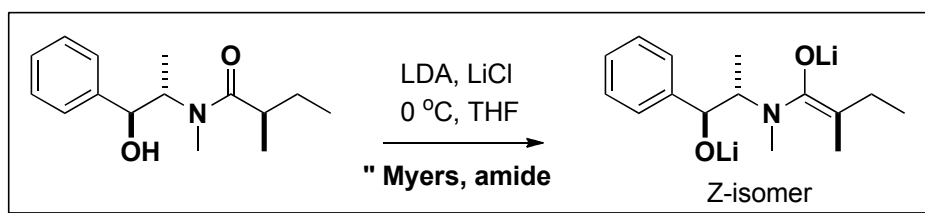
series	$n$	$m$	lactam	$R_1$	$R_2$	O-C-C-S dihedral <sup>a</sup>	Z/E ratio <sup>b</sup>	lactam	$R_1$	$R_2$	O-C-C-S dihedral <sup>a</sup>	Z/E ratio <sup>b</sup>
1	1	1	4a	<i>n</i> -Pr	Me	174	47:53	4b	Me	<i>n</i> -Pr	182	64:36
2	1	1	4c	Allyl	Me	175	44:56	4d	Me	Allyl	178	68:32
3	1	2	5a	<i>n</i> -Pr	Me	141	87:13	5b	Me	<i>n</i> -Pr	128	20:80
4	1	2	5c	Allyl	Me	140	87:13	5d	Me	Allyl	138	26:74
5	1	2	5e	Bn	Me	145	92:8	5f	Me	Bn	149	12:88
6	1	2	5g	<i>n</i> -Pr	Et	139	80:20	5h	Et	<i>n</i> -Pr	137	12:88
7	2	2	6a	<i>n</i> -Pr	Me	140	83:17	6b	Me	<i>n</i> -Pr	133	37:63
8	2	2	6e	Bn	Me	143	92:8	6f	Me	Bn	139	53:47

<sup>a</sup> Weighted average (calculated at  $-78^\circ\text{C}$ ) of all conformations within 2 kcal/mol of the ground state as determined by Monte Carlo calculations.

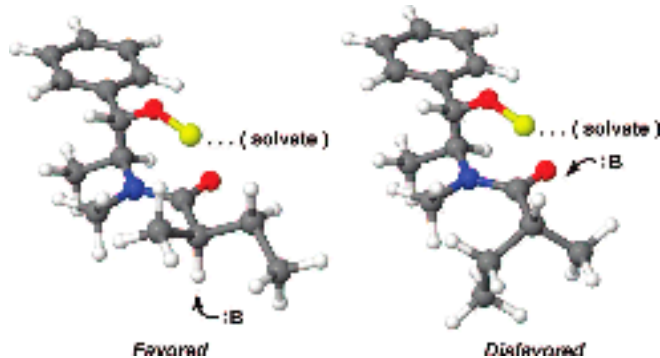
<sup>b</sup> Determined by integration of  $^{13}\text{C}$  resonances.

⇒ The method affords both *E*- and *Z*-amide enolates without relying on a steric difference between the two substituents.

## iii) Stereocontrolled Alkylative Construction of Quaternary Carbon Centers

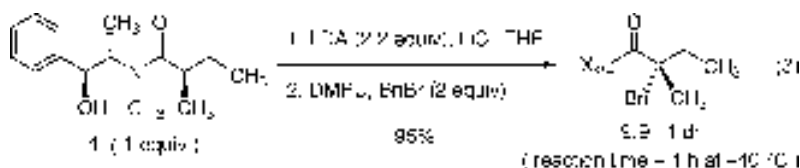


A. G. Myers, JACS, 2008, 130, 13231.

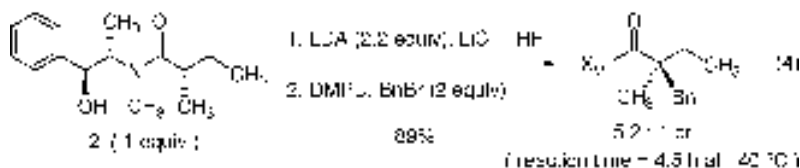


They propose that in the favored pretransition state assemblies the alkoxide side chain and base are positioned on opposite faces of the incipient enolate, with the  $\alpha$ -C-H bond aligned for deprotonation.

Proposed pretransition state assemblies leading to favored (*Z*) and disfavored (*E*) geometric enolate isomers by sequential deprotonations of pseudoephedrine amide.



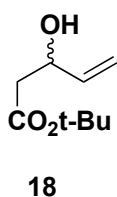
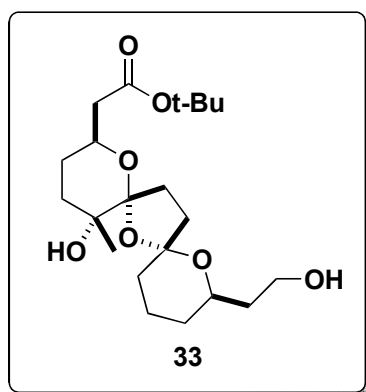
The electrophile is proposed to approach the enolate  $\pi$ -face opposite the alkoxide side chain. Benzylation of the *Z*-enolate is both more diastereoselective and more rapid than benzylation of the *E*-enolate.



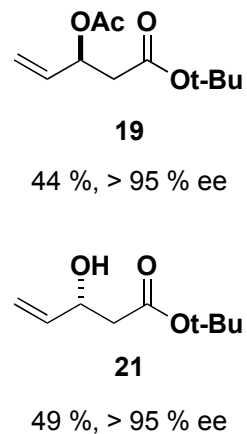
*Z*- and *E*- $\alpha$ -methyl- $\alpha$ -ethyl disubstituted pseudoephedrine amide enolates are alkylated preferentially from a common diastereoface.



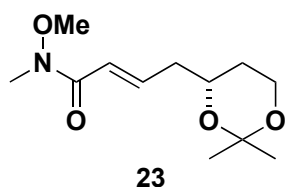
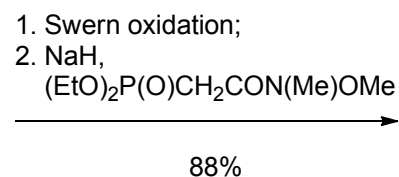
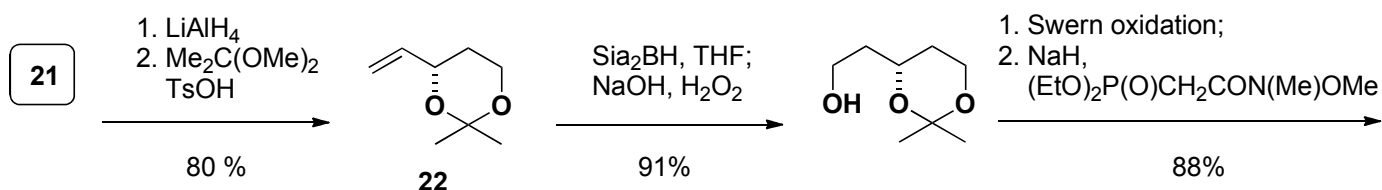
## Synthesis of BCD-Bisketal Fragment 33



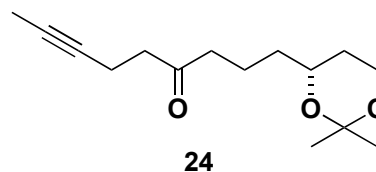
Aminolipase PS-D,  
vinylacetate, pentane  
30 °C



Acylation of racemic alcohol **18** was terminated at 50 % conversion, and the products were separated by column chromatography.

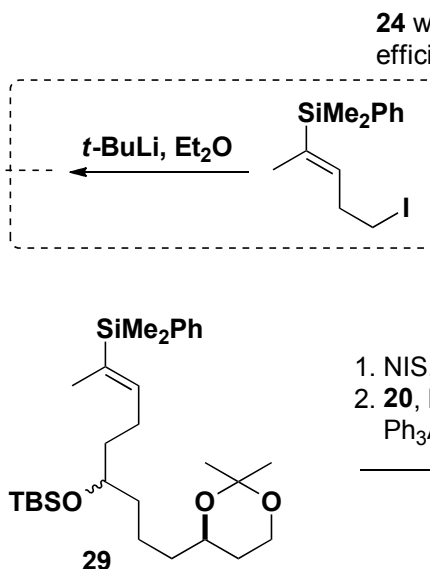


1. 10 % Pd/C, H<sub>2</sub>, EtOAc;  
2. MeC≡CCH<sub>2</sub>CH<sub>2</sub>MgBr, THF

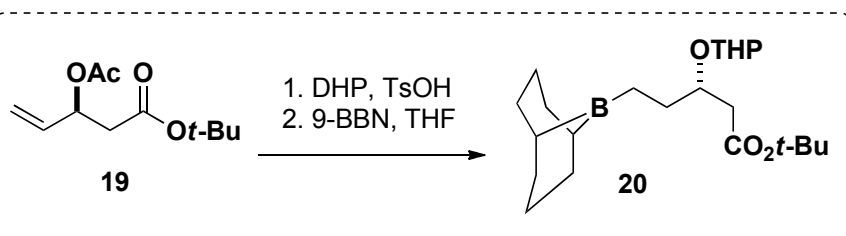
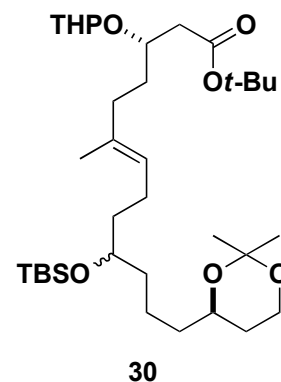


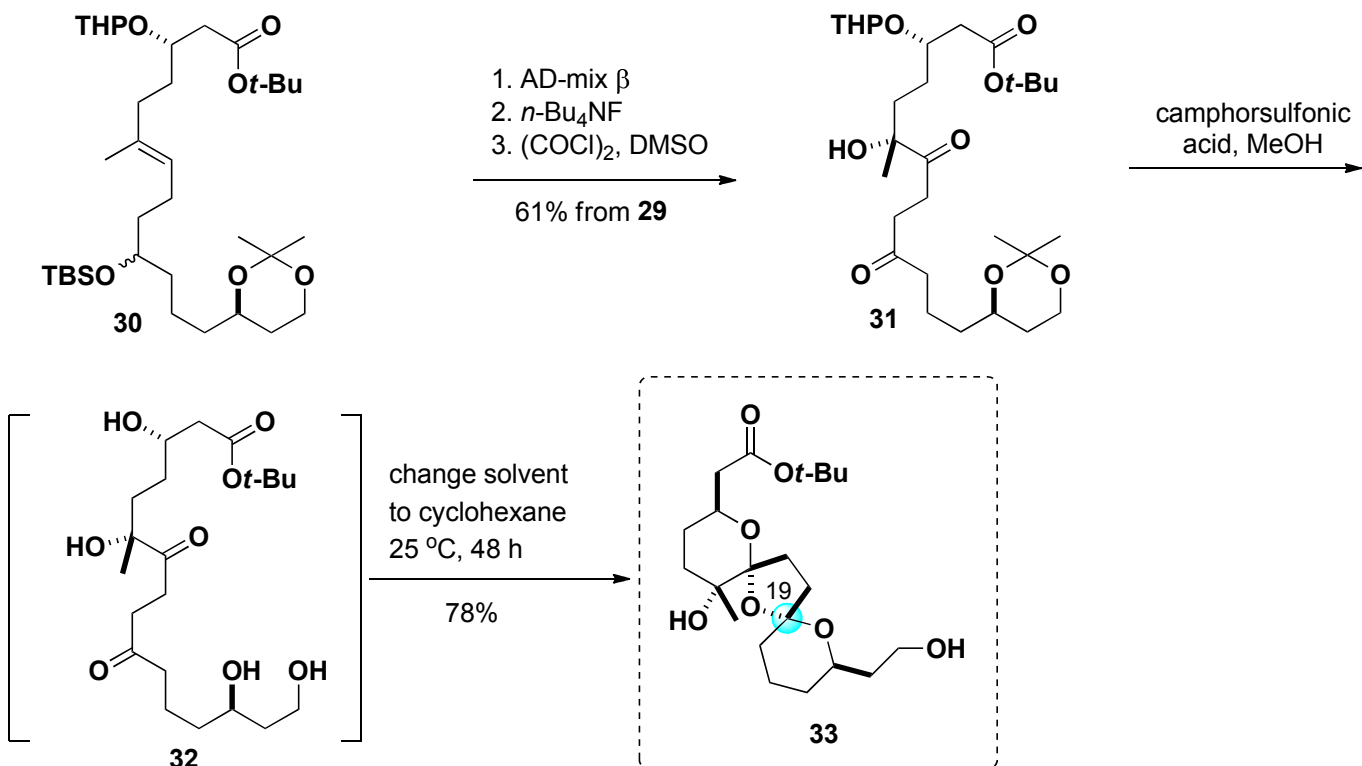
1. 10 % Pd/C, H<sub>2</sub>, EtOAc  
2.   
**28**, THF  
3. NaBH<sub>4</sub>, MeOH; 97%  
4. TBSCl, imidazole; 99%

90% from **23**

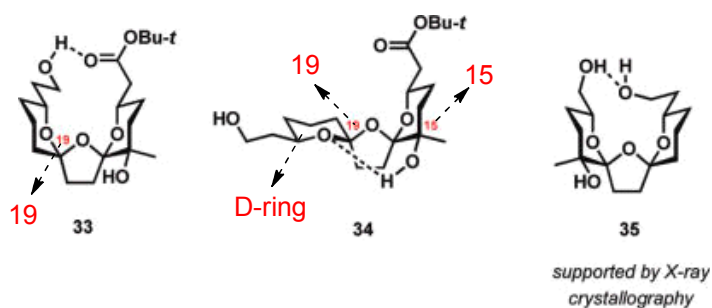


1. NIS, (CF<sub>3</sub>)<sub>2</sub>CHOH  
2. **20**, Pd(dppf)Cl<sub>2</sub>, Ph<sub>3</sub>As, Cs<sub>2</sub>CO<sub>3</sub>





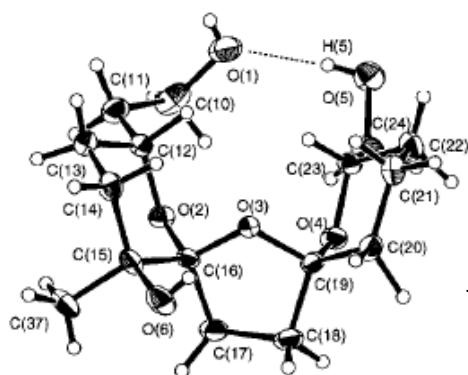
### Hydrogen-bonding stabilization in spiroketal intermediates



Upon superficial analysis, isomer **33** fully stabilized by anomeric effect should be increasingly more favored over its epimer **34** lacking anomeric stabilization at C19 as the medium polarity

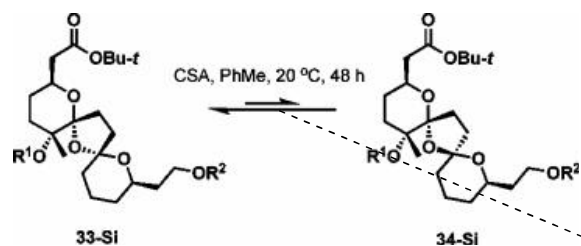
The C19 epimer **34** can be stabilized by a hydrogen bond between the tertiary hydroxy group at C15 and the D-ring oxygen, while the desired isomer is stabilized by long-range hydrogen bonding between the terminal ester and hydroxyl groups. The unusual long-range hydrogen bonding is supported by crystallographic studies.

SYNLETT, 1997, 18, 298.



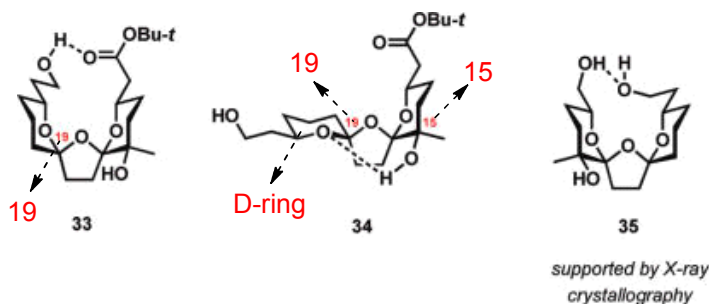
The structure of **35** was unambiguously established by X-ray analysis, which indicates the existence of an intermolecular hydrogen bond between the terminal diol groups. This hydrogen bond must play an important role in stereoselective formation of **35** in toluene.

## Effect of Selective Silylation on Relative Stability of C19 Epimers



entry	R <sup>1</sup>	R <sup>2</sup>	33-Si:34-Si
1	H	H	4.0:1
2	H	<i>i</i> -Pr <sub>3</sub> Si	1.7:1
3	Et <sub>3</sub> Si	H	13:1
4	Et <sub>3</sub> Si	<i>i</i> -Pr <sub>3</sub> Si	8.3:1

Upon extended reaction times, the desired diastereomer 33 is produced as a major product; however, the C19 epimer is formed initially and thus is favored under kinetic control.



In order to further ascertain the effect of hydrogen bonding on the selectivity of spiroketalization,

They carried out equilibration experiment with selectively silylated substrates. In all cases, the desired configuration at C19 was favored, but the level of preference varied substantially.

As shown the Table, silylation of the tertiary hydroxyl group (Et<sub>3</sub>Si) increased the ratio significantly to 13:1 (entry 3).

⇒ These results indicate that when only the anomeric effect is operational in the fully silylated substrate (entry 3), the thermodynamic ratio of 8.3:1 is observed in toluene, and hydrogen bonding from both tertiary and primary and primary hydroxyl groups has a significant effect on the position of the equilibrium.

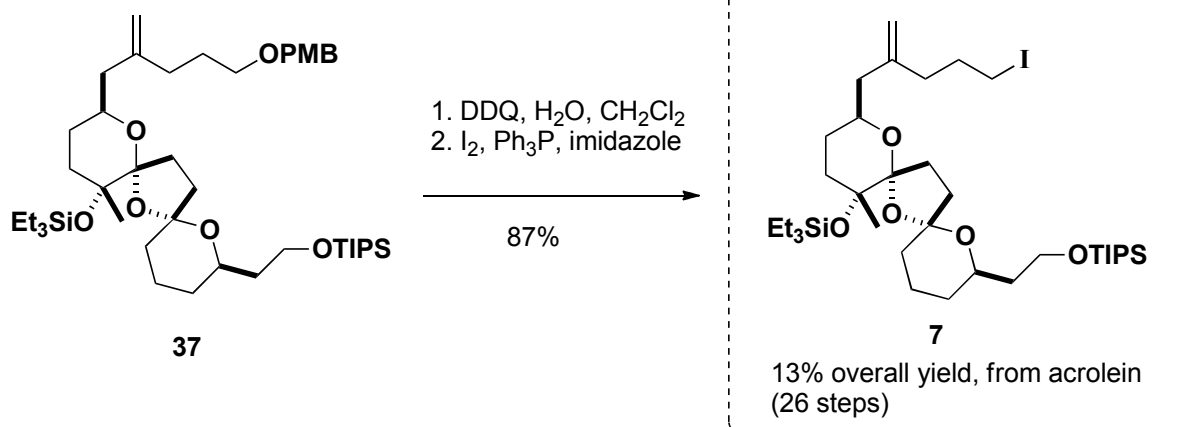
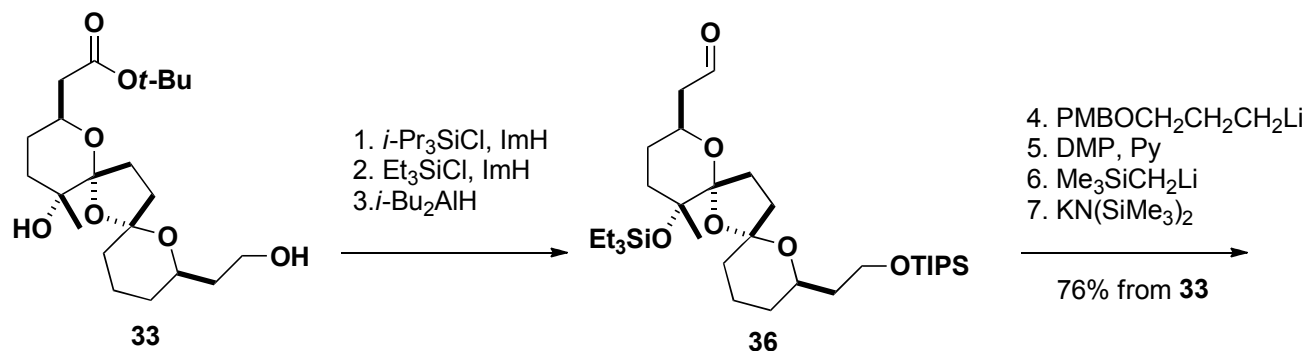
## Solvent Effect on the Spiroketalization

Table 1. Solvent Effect on the Spiroketalization

entry	solvent	isolated yield (%)	
		16	17
1	methanol	49	22
2	dichloromethane	62	23
3	toluene	63	13
4	cyclohexane	78	8

As the solvent polarity decreased, we observed an increased ratio of the desired diastereomer to its C19 epimer. And the optimal selectivity (9.8:1) was achieved when cyclohexane was used as the solvent.

## Construction of fragment 7



## Completion of PnTX A

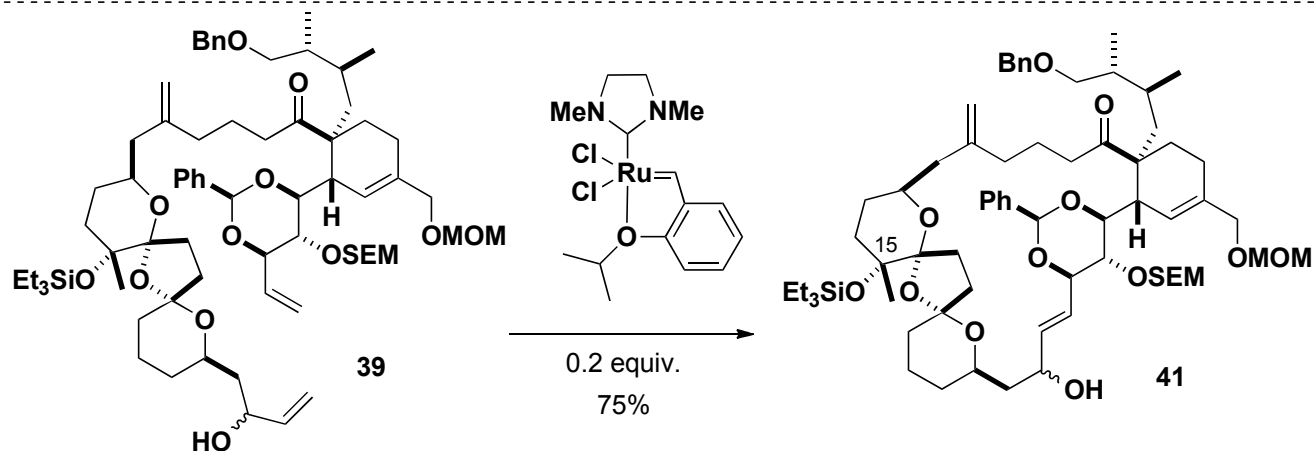
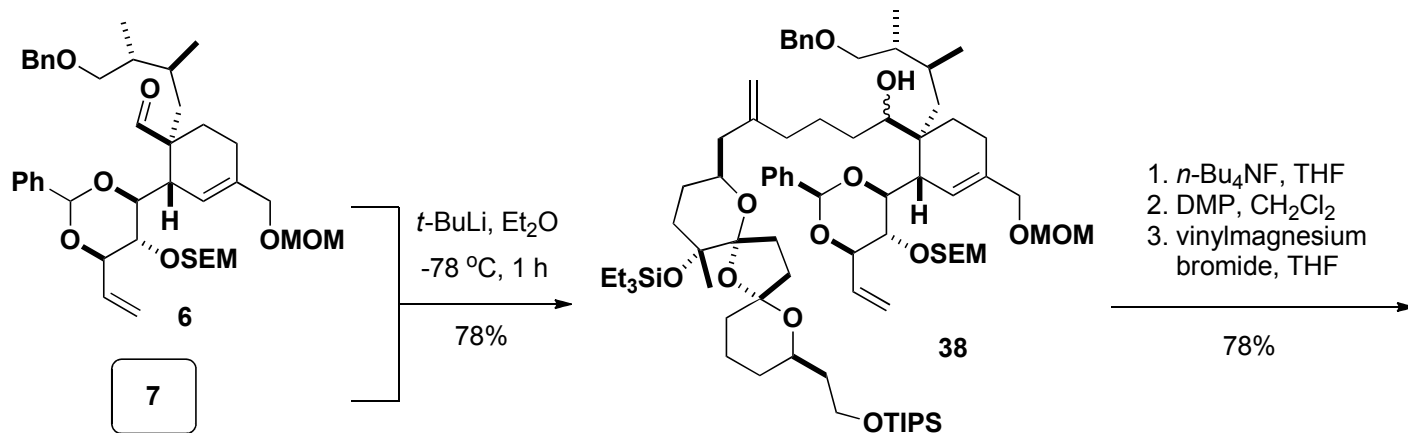




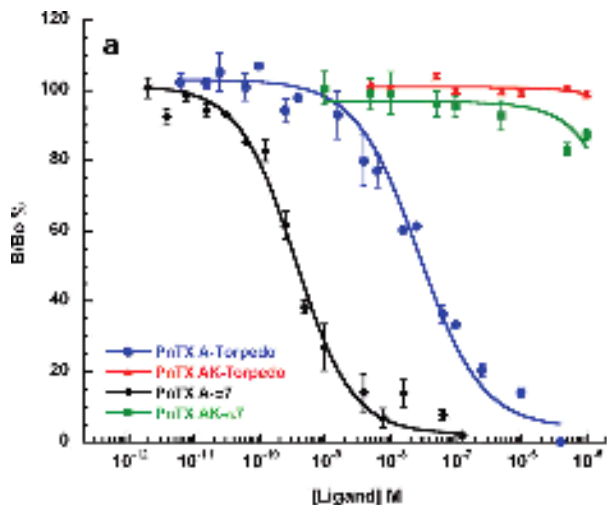
**Table 2. Inhibition Constants for PnTX A on ACh-Evoked Nicotinic Currents in *Xenopus* Oocytes<sup>a</sup>**

nAChR	PnTX A IC <sub>50</sub> <sup>b</sup> (nM)
$\alpha 7$ (human)	0.107 (0.086–0.132)
$\alpha 4\beta 2$ (human)	30.1 (19.4–47.5)
$\alpha 1_2\beta\gamma\delta$ ( <i>Torpedo</i> )	5.55 (4.5–6.8)

**a:** Oocytes expressed human neuronal  $\alpha 7$  or  $\alpha 4\beta 2$  nAChR subtypes or were microtransplanted with muscle-type  $\alpha 1_2\beta\gamma\delta$  nAChR.

**b:** Mean values from concentration-response curves were recorded on 46–50 oocytes for each experimental condition; 95% confidence intervals are shown in parentheses.

**ii) Binding Competition Experiments between PnTX A and Radiolabeled Ligands**



**Effect of PnTX A and AK on various nAChRs.**

Inhibition of specific [<sup>125</sup>I]  $\alpha$ -bungarotoxin or ( $\pm$ )-[<sup>3</sup>H]epibatidine binding by increasing concentrations of PnTX A or AK on (a) *Torpedo* and neuronal  $\alpha 7$ -5HT<sub>3</sub> or (b) heteropentameric  $\alpha 3\beta 2$  and  $\alpha 4\beta 2$  nAChRs.

The results are expressed as the ratio of the specific radiotracer binding measured with (B) or without (B<sub>0</sub>) competitive ligands, expressed as a percentage.

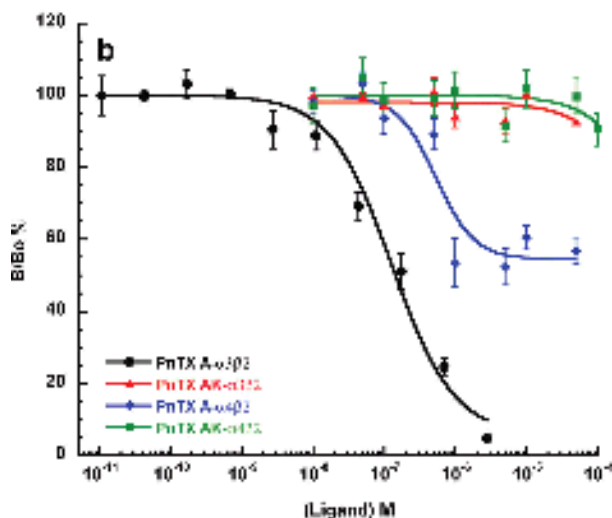


**Table 3. Affinity Constants for PnTX A and Its Amino Keto Analogue (PnTX AK) on Muscle and Neuronal nAChR Subtypes<sup>a</sup>**

ligand	K <sub>i</sub> ± SEM <sup>b</sup> (nM)			
	$\alpha 1_2\beta\gamma\delta$ ( <i>Torpedo</i> )	$\alpha 7$ -5HT <sub>3</sub> (chick)	$\alpha 4\beta 2$ (human)	$\alpha 3\beta 2$ (human)
PnTX A	2.8 ± 0.03	0.35 ± 0.04	15.6 ± 5.3	9.4 ± 1.9
PnTX AK	>1000	>10000	>2000	>2000

<sup>a</sup>Determined by equilibrium competition binding experiments. <sup>b</sup>Mean values ± SEM from three distinct experiments performed in duplicate.



PnTX A binds to these receptors with affinities in nanomolar range, and its order of potency on the various nAChRs subtypes is  $\alpha 7$ -5HT<sub>3</sub> > *Torpedo* >  $\alpha 3\beta 2$  =  $\alpha 4\beta 2$ .

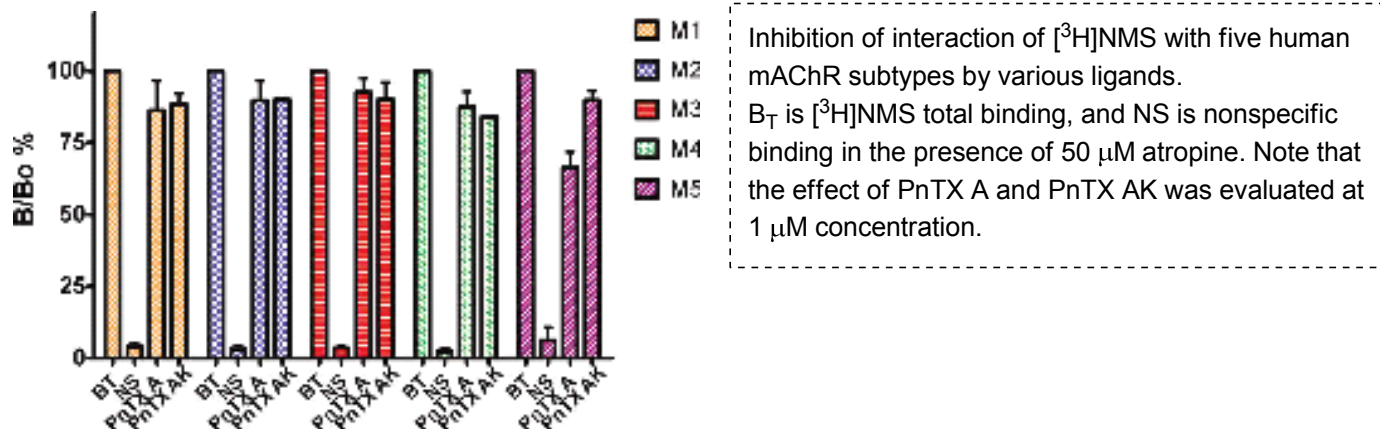


Studies on the binding potency of PnTX AK on the nAChRs subtypes showed that this toxin produces no significant displacement of the radioactive tracer, even at high concentrations.



Thus, disruption of the imine ring in PnTX A is responsible for the drastic loss of affinity of this compound for the various nAChR subtypes.

iii) Potential inhibitory activity of 1  $\mu\text{M}$  PnTX A or PnTX AK was evaluated on CHO cells stably expressing the distinct human muscarinic acetylcholine receptor (mAChR) subtypes



⇒ As shown here, both PnTX A and PnTX AK had no significant effect on  $^3\text{H}$ -NMS binding to M1, M2, M3 and M4 mAChR subtypes, whereas PnTX A induced 35% radiotracer displacement in M5 mAChR, indicating a low micromolar affinity for this receptor subtype.

## Summary

### Pinnatoxin A: Selective Inhibition of nAChRs

Indeed, until now, the mode of action of pinnatoxins was ascribed to action on calcium channels. However, in this studies, even at 10  $\mu\text{M}$  PnTX A, no significant binding activity was detected for calcium channels.

Toxicological profile is also seen with agents affecting nicotinic receptors.

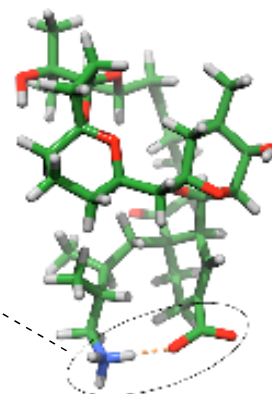
### [The reason of the inactivity of PnTX AK with nAChRs]

This inactivity can be explained by the existence of conformers strongly stabilized by an intramolecular ionic interaction between the ammonium and carboxylate groups of PnTX AK in solution.

### [The cyclic imine moiety represents the key feature in this family of toxin]

1) In conjunction with the C28 hydroxy groups of the bridged EF-ketal, it anchors the ligand to the binding site through hydrogen bonds in a conformation ideally positioned to optimize the interactions with neighboring residues.

2) Binding of the closed imino ring A in PnTX A appears to be more favorable, both sterically and energetically, than that of the corresponding open amino ketone form in PnTX AK. The functional signature in the cyclic imine phycotoxins, interacting with nicotinic receptors as has been shown for PnTX A.



Finally, aside from their clear effect on nAChRs, interaction of cyclic amine toxins with other targets of the cholinergic neurotransmission pathway, especially the muscarinic receptors (mAChRs), has also been reported recently. Although no interaction was observed with M1-4 mAChRs subtypes, a weak effect of PnTX A was measured for the M5 subtype, suggesting a low micromolar affinity of this toxin for the M5 receptor subtype.